Using Meander Open Complementary Split Ring Resonator (MOCSRR) Particles to Design a Compact UHF RFID Tag Antenna

Benjamin D. Braaten, *Member, IEEE*, and Masud A. Aziz, *Student Member, IEEE*

***Abstract*—In this letter, a new printed dipole that uses series-connected meander open complementary split ring resonator (MOCSRR) particles is introduced. It is shown that by using the antenna presented here on a prototype passive UHF radio frequency identification (RFID) tag, useful read ranges up to 4.1 m can be achieved. The printed dipole on the prototype resonates at an overall dimension of approximately $0.1\lambda_0$, where λ_0 is the free-space wavelength at resonance. The equivalent circuit of each MOCSRR particle is extracted and compared to the equivalent circuit of an open complementary split ring resonator (OCSRR) particle with the same overall dimensions and an OCSRR particle with larger overall dimensions. It is shown that the MOCSRR particle resonates at a lower frequency than both of the OCSRR particles, thus contributing to the lower resonant frequency of the antenna. The read range of the prototype is comparable to other passive UHF RFID tags with dimensions that are up to twice the overall size.**

***Index Terms*—Dipole, meander, open complementary split ring resonator (OCSRR) and passive tag, radio frequency identification (RFID).**

I. Introduction

PASSIVE UHF radio frequency identification (RFID) tags typically consist of a printed antenna, a passive integrated circuit (IC) and a thin flexible substrate [1]. When designing a printed antenna for a passive UHF RFID tag, it is usually very desirable for the overall dimensions of the antenna to be as compact as possible while preserving the performance of the tag. Because of such constraints on the dimensions of the RFID tag, many novel antenna designs have been proposed [1]–[3]. A very popular type of antenna for a RFID tag is the space-filling meander-line antenna [2], [3] shown in Fig. 1. Each dipole arm consists of several series-connected vertical conductors (i.e., conductors in the y-direction) printed on a single ungrounded dielectric substrate. The current on each vertical conductor is in the opposite direction of the current on each adjacent vertical conductor. This results in a canceled far field from these elements. Thus, the radiation from the meander-line dipole is mainly due to the small horizontal segments (i.e., the segments in the x-direction) connecting each vertical segment.

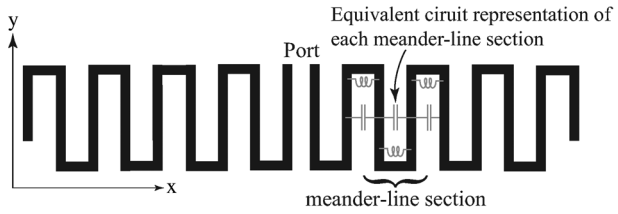

Fig. 1. Meander-line antenna with the equivalent circuit elements shown in gray.

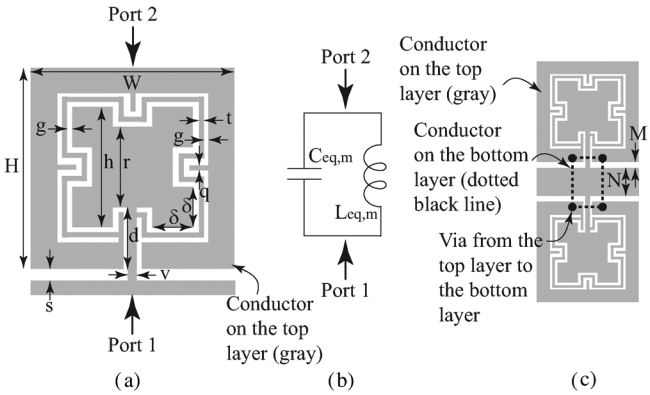

Fig. 2. (a) Meander open complementary split ring resonator particle (MOCSRR). (b) Equivalent circuit of the MOCSRR particle. (c) CPW structure used to determine the resonant frequency of the MOCSRR particle using momentum and measurements.

The equivalent circuit for each meander-line section is also shown in Fig. 1. The long vertical traces contribute to the capacitance of each meander-line section, while the short horizontal segments contribute to the inductance of each meander-line section. Thus, the equivalent circuit for each meander-line section is a capacitor in parallel with an inductor [4]. It is these meander-line sections that contribute to the lower resonant frequency of the meander-line antenna.

This letter introduces a recently developed printed dipole designed using the meander open complementary split ring resonator (MOCSRR) particle shown in Fig. 2(a) [5]. In particular, each pole of the dipole is formed using series-connected MOCSRR particles in the manner shown in Fig. 3(a). The MOCSRR particle used here is a modification of the recently published coplanar waveguide (CPW) open complementary spit ring resonator (OCSRR) particle in [6]. Instead of the concentric rings used in the OCSRR particle, the MOCSRR particle uses a meander-line path [7]. The equivalent circuit of

Manuscript received May 21, 2010; revised July 13, 2010 and August 11, 2010; accepted September 29, 2010. Date of publication October 25, 2010; date of current version November 18, 2010.

The authors are with the Department of Electrical and Computer Engineering, North Dakota State University, Fargo, ND 58105 USA (e-mail: benbraaten@ieee.org).

Color versions of one or more of the figures in this letter are available online at http://ieeexplore.ieee.org.

Digital Object Identifier 10.1109/LAWP.2010.2089421

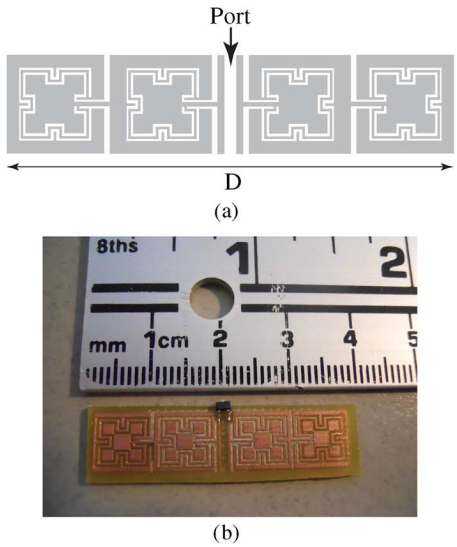

Fig. 3. (a) MOCSRR-based UHF RFID antenna. (b) MOCSRR UHF RFID prototype tag ($D = 36.24$ mm, $W = 8.2$ mm, $H = 8.05$ mm, $s = 0.42$ mm, $v = 0.22$ mm, $d = 2.92$ mm, $h = 5.17$ mm, $r = 2.25$ mm, $t = 0.33$ mm, $g = 0.31$ mm, $\delta = 1.54$ mm, and $q = 0.43$ mm).

the MOCSRR particle is a capacitor in parallel with an inductor, which is the same equivalent circuit of the OCSRR particle. The equivalent inductance is created by the meander ring in the slot connecting port one with port two, and the equivalent capacitance is a result of the meander slots between the meander ring and the outer conducting planes. The equivalent circuit of each MOCSRR particle is the same as the equivalent circuit of each meander-line section in Fig. 1. Therefore, by connecting the MOCSRR particles in series, the resonant frequency of a small printed dipole can be reduced in a manner similar to the meander-line antenna.

This letter is organized as follows. In Section II, the new printed dipole with series-connected MOCSRR particles is presented by designing a prototype UHF RFID tag. Next, several equivalent circuits are extracted for various MOCSRR and OCSRR particles. These equivalent circuits are then compared and discussed, and finally, conclusions are presented in Section III.

II. MOCSRR UHF RFID Tag Antenna

For application purposes, the prototype RFID tag was designed to be attached to the plastic bottle cap of an empty beverage container. This required the prototype tag to be very small and still have a useful read range. The Higgs-2[1] by Alien Technology [8] was chosen as the passive IC on the RFID tag. At 920 MHz, the Higgs-2 IC has an input impedance of $Z_{\rm IC} = 13.73 - {\rm j}142.8\ \Omega$ [8]. Therefore, the antenna on the tag should have an input impedance near the conjugate of $Z_{\rm IC}$ for sufficient power delivery to the passive IC. These requirements resulted in the layout of the prototype tag with the new MOCSRR antenna shown in Fig. 3(b). The antenna in Fig. 3(b) was designed in Momentum [9] with a 1.36-mm-thick FR-4 substrate ($\varepsilon = 4.2$ measured and $\tan\delta = 0.011$ measured).

[1]The sensitivity during a read is -14 dBm, and the sensitivity during programming is -10 dBm. Also, the equivalent input impedance is a 1.5-kΩ resistor connected in parallel with a 1.2-pF capacitor [8].

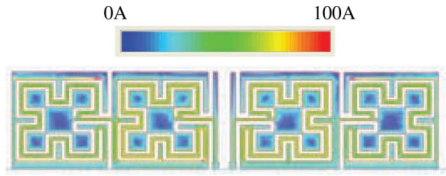

Fig. 4. Simulated surface currents on the printed MOCSRR antenna.

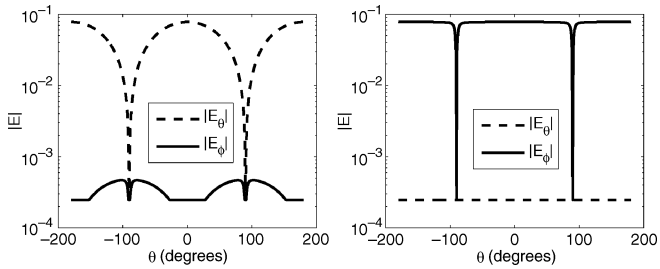

Fig. 5. Simulated far-field patterns in the xz plane (left) and the yz plane (right).

It should be mentioned that several design iterations lead to the antenna on the prototype tag in Fig. 3(b). There are two reasons for this. First, the modeling software, Momentum, is restricted to planar structures. The RFID tag was being applied to a three-dimensional problem that was approximated in Momentum. Second, the material properties of the plastic cap were unknown. Even with these uncertainties, a gain of 0.917 dBi and an input impedance of $8.2 + j195.0\ \Omega$ were simulated without modeling the plastic bottle cap in Momentum.

A. Measured Read Range of the Prototype RFID Tag

Next, the read range of the prototype tag was measured to determine how well the antenna was matched with the input impedance of the Higgs-2 passive IC on the tag. To do this, an Alien Technology 9780 reader [8] (with a maximum output power of 1 W) connected to a CP antenna with a gain of 6 dBi and the prototype tag on the plastic bottle were placed in an anechoic chamber. A max read range of 4.11 m was measured. This long read range indicates that a good match between the MOCSRR antenna and the input impedance of the Higgs-2 IC was obtained by attaching the tag to the plastic container. As a comparison, the read range of the larger meander-line antenna reported in [10] on a plastic container was 3.5 m. The read range of the prototype tag reported in this work is longer, and the overall size is 57.4% smaller than the prototype tag reported in [10].

Also, the surface currents on the printed antenna were computed using Momentum and are shown in Fig. 4. Furthermore, the far-field patterns in the xz and yz planes were computed using Momentum and are shown in Fig. 5.

B. Extracting the Equivalent Circuit of the MOCSRR Particle

Next, to provide insight on the behavior of the MOCSRR dipole, the equivalent circuit of the MOCSRR particle shown in Fig. 2(b) was extracted. The CPW structure in Fig. 2(c) was used to extract the equivalent circuit of the MOCSRR particle (the same CPW structure was used in [6] to extract the equivalent circuit of the OCSRR particle). The dimensions of the MOCSRR particle in Fig. 2(c) are the same as the dimensions

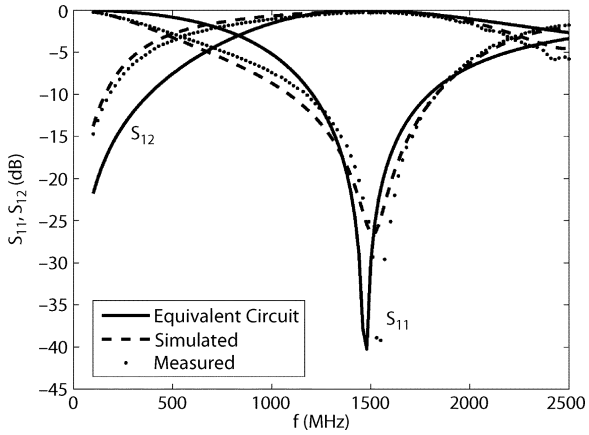

Fig. 6. S-parameters of the MOCSRR particle.

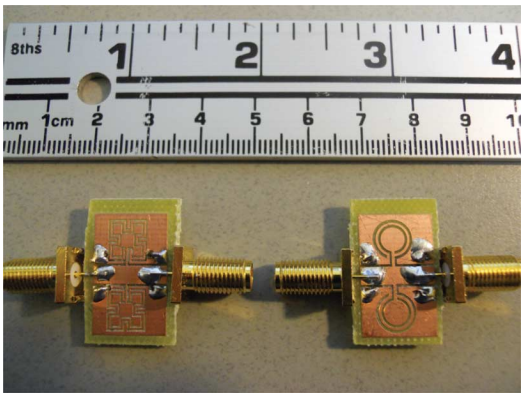

Fig. 7. (Left) Manufactured MOCSRR particle and (Right) manufactured OCSRR particle on the same ungrounded FR4 substrate as the prototype RFID tag ($M = 0.4$ mm and $N = 3.1$ for both).

of each particle used in the antenna design on the prototype tag (Fig. 3). First, the CPW structure in Fig. 2(c) was modeled in Momentum [9] (with the same substrate as the prototype RFID tag). The S-parameters for these simulations are shown in Fig. 6. When the MOCSRR particle resonates, the impedance on the CPW line caused by the particle approaches infinity. Therefore, when S_{11} is the lowest, the particles in Fig. 2(c) are resonating. The simulated resonant frequency was $f_{\mathrm{m,sim}} = 1.55$ GHz.

Next, using a curve-fitting technique (similar to the approach used in [6]), the equivalent circuit of the MOCSRR particle was determined. The inductance and capacitance values in Fig. 2(b) were computed to be $L_{\mathrm{eq,m}} = 3.75$ nH and $C_{\mathrm{eq,m}} = 3.1$ pF, respectively. Further discussion on the equivalent circuit extraction can be found in [6]. The S-parameters for the extracted equivalent circuit compare well to the simulations in Fig. 6. Next, the CPW structure in Fig. 2(c) was manufactured, and the S-parameters were measured using an Agilent Technologies 4.5-GHz E5071C ENA series network analyzer. The printed MOCSRR CPW structure is shown in Fig. 7 (left side). The measured S-parameters are also shown in Fig. 6. The measured resonant frequency was $f_{\mathrm{m,meas}} = 1.52$ GHz.

In all cases, the S-parameters compare very well. At 920 MHz, the MOCSRR particle has an impedance of $Z_{\mathrm{mocsrr}} = j30.8\ \Omega$. This shows that the inductance of the MOCSRR particle is dominant. Since the input impedance of

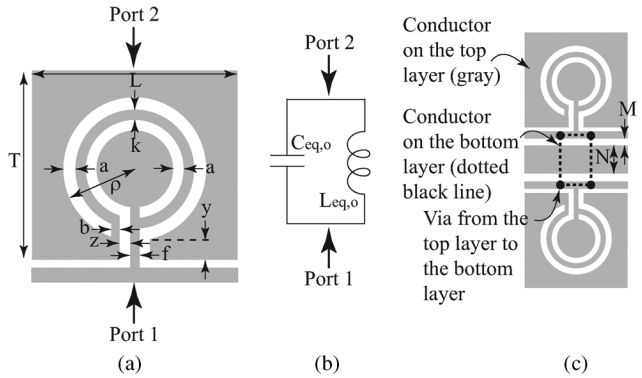

Fig. 8. (a) Dimensions of the OCSRR. (b) Equivalent circuit of the OCSRR particle. (c) CPW structure used to determine the resonant frequency of the OCSRR particle using Momentum and measurements ($L = 8.3$ mm, $T = 8.1$ mm, $a = 0.51$ mm, $b = 0.46$ mm, $f = 0.47$ mm, $k = 0.45$ mm, $\rho = 3.5$ mm, $y = 0.97$ mm, and $z = 0.39$ mm).

an electrically small antenna is typically capacitive [4], this provides insight as to why the dipole on the prototype tag resonates at an overall dimension around $0.1\lambda_0$, where λ_0 is the free-space wavelength at resonance.

C. Extracting the Equivalent Circuit of the OCSRR Particle

Next, the equivalent circuit of the OCSRR particle in Fig. 8(a) was extracted. This was done to compare the equivalent circuit of the OCSRR particle [Fig. 8(b)] introduced in [6] to the MOCSRR particle used in this letter. Using the CPW structure shown in Fig. 8(c), the same overall dimensions of MOCSRR particle used in the antenna design shown in Fig. 3(b), and the same substrate as the prototype RFID tag, an equivalent circuit of $L_{\mathrm{eq,o}} = 1.5$ nH and $C_{\mathrm{eq,o}} = 3.2$ pF was extracted using Momentum. The resonant frequency of the particle was $f_{\mathrm{o,sim}} = 2.32$ GHz. Finally, the CPW structure in Fig. 8(c) was manufactured, and the S-parameters were measured. The printed OCSRR CPW structure is shown in Fig. 7 (right side). The measured resonant frequency was $f_{\mathrm{o,meas}} = 2.28$ GHz. The S-parameters compared well in all three cases (simulated, equivalent circuit, and measured). The results here show that the inductance of the MOCSRR particle is approximately twice the inductance of the OCSRR particle.

Next, the equivalent circuit of the larger OCSRR particle used in the antenna design for the prototype RFID tag presented in [11] was extracted. Using the CPW structure shown in Fig. 8(c), the dimensions of OCSRR particle defined in [11], and the same substrate as the prototype RFID tag, an equivalent circuit of $L_{\mathrm{eq,o,[11]}} = 4.2$ nH and $C_{\mathrm{eq,o,[11]}} = 2.0$ pF was extracted using Momentum. The resonant frequency of the particle was $f_{\mathrm{o,sim,[11]}} = 1.8$ GHz. At 920 MHz, the OCSRR particle has an impedance of $Z_{\mathrm{ocsrr}} = j33.7\ \Omega$, which is comparable to Z_{mocsrr} of the much smaller prototype tag.

D. Characteristics of the MOCSRR Particle

The equivalent circuit of the MOCSRR particle used on the prototype tag was computed next for various particle dimensions. First, the ring gap dimension g in Fig. 2(a) was changed on an individual MOCSRR particle, and the equivalent circuit was extracted using Momentum. The results from these simulations are summarized in Table I. Next, the ring gap was fixed at

TABLE I
EQUIVALENT CIRCUIT FOR VARIOUS PARTICLE DIMENSIONS

g (mm)	δ (mm)	L_{eq} (nH)	C_{eq} (pF)	f_o (GHz)
0.31	1.14	3.7	2.85	1.54
0.31	1.24	3.6	2.95	1.54
0.31	1.34	3.4	3.15	1.53
0.31	1.44	3.5	3.1	1.52
0.31	1.54	3.75	3.1	1.47
0.31	1.64	3.8	3.15	1.45
0.31	1.54	3.75	3.1	1.47
0.21	1.54	3.3	3.7	1.41
0.11	1.54	3.5	3.85	1.37

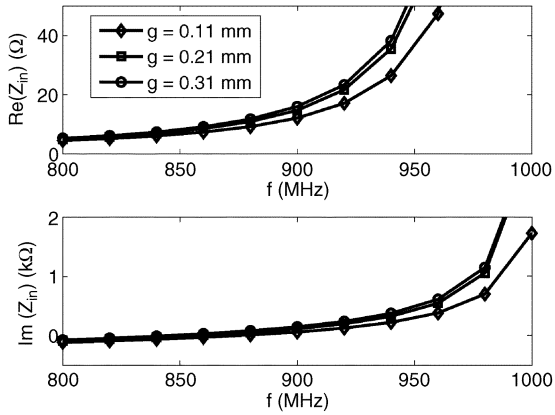

Fig. 9. Simulated input impedance on the FR-4 substrate for various ring gap values g (the value of t was fixed for these computations).

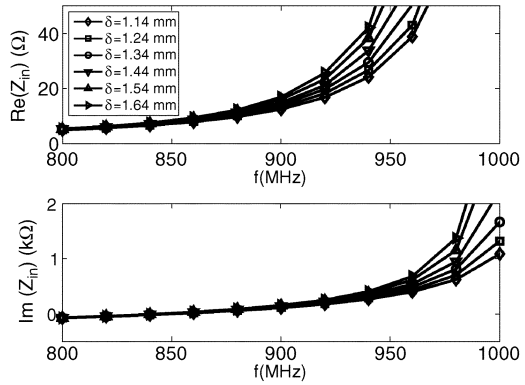

Fig. 10. Simulated input impedance on the FR-4 substrate for various values of δ (the values of t and g were fixed for these computations).

0.31 mm, and δ in Fig. 2(a) was changed. Then, the equivalent circuit of the MOCSRR particle was determined for the various values of δ. The results from these computations are also shown in Table I. Finally, the input impedance of the antenna on the prototype RFID tag was computed for several ring gap dimensions g and various values of δ. The results from these simulations are shown in Figs. 9 and 10.

The following useful comments can be made about the results in Table I and Figs. 9 and 10.

1) The results in Table I show how the resonant frequency of an individual particle can be increased by increasing the width of the ring gap g. In particular, the results in Table I show how g is related to the equivalent capacitance of the MOCSRR particle. As g is reduced, the capacitance of the equivalent circuit is increased. This is expected because the distance between the inner meander ring and the surrounding conducting planes is being reduced, thus resulting in a larger capacitance.
2) The results in Table I show the relation between the resonant frequency of the MOCSRR particle and the value of δ.
3) The results in Fig. 9 show how both the real and imaginary parts of the input impedance of the prototype antenna are affected by various ring gap dimensions g.
4) The results in Fig. 10 are particularly useful. These results show how the input impedance of the antenna is related to the values of δ. As the values of δ are changed, the real part of the input impedance of the antenna at 920 MHz can be modified to match the input impedance of the IC on the tag. This is very useful for a designer because the imaginary part of the input impedance of the antenna tends to change much less for various values of δ. This is interesting because many geometric changes to an antenna tend to effect both the real and imaginary parts of the input impedance of an antenna [10].

III. CONCLUSION

A new printed dipole design on a passive UHF RFID tag that uses series-connected meander open complementary split ring (MOCSRR) resonator particles has been presented. The equivalent circuit of various MOCSRR particles were extracted and compared to the equivalent circuit of published OCSRR particles. The relation between the equivalent circuit and the dimensions of the MOCSRR particle is also summarized. Furthermore, the input impedance of the antenna on the prototype RFID tag was computed for various MOCSRR particle dimensions.

REFERENCES

[1] K. Finkenzeller, *RFID Handbook: Fundamentals and Applications in Contactless Smart Cards and Identification*. West Sussex, England: Wiley, 2003.
[2] H.-D. Chen and Y.-H. Tsao, "Low-profile PIFA array antennas for UHF band RFID tags mountable on metallic objects," *IEEE Trans. Antennas Propag.*, vol. 58, no. 4, pp. 1087–1092, Apr. 2010.
[3] C. Calabrese and G. Marrocco, "Meander-slot antennas for sensor-RFID tags," *IEEE Antennas Wireless Propag. Lett.*, vol. 7, pp. 5–8, 2008.
[4] R. Bancroft, *Microstrip and Printed Antenna Design*. Raleigh, NC: Scitech, 2006, pp. 194–195.
[5] B. D. Braaten, M. A. Aziz, M. J. Schroeder, and H. Li, "Meander open complementary split ring resonator (MOCSRR) particles implemented using coplanar waveguides," in *Proc. IEEE Int. Conf. Wireless Inf. Technol. Syst.*, Honolulu, HI, Aug. 28–Sep. 3, 2010, pp. 1–4.
[6] A. Velez, F. Aznar, J. Bonache, M. C. Valazquez-Ahumada, J. Martel, and F. Martin, "Open complementary split ring resonators (OCSRRs) and their application to wideband CPW band pass filter," *IEEE Microw. Wireless Compon. Lett.*, vol. 19, no. 4, pp. 197–199, Apr. 2009.
[7] G.-L. Wu, W. Mu, X.-W. Dai, and Y.-C. Jiao, "Design of novel dual-band bandpass filter with microstrip meander-loop reonator and CSRR DGS," *Prog. Electromagn. Res.*, vol. PIER 78, pp. 17–24, 2008.
[8] "Alien Technology," Alien Technology, Morgan Hill, CA [Online]. Available: http://www.alientechnology.com
[9] "Advanced Design System—ADS 2009," Agilent Technologies, Santa Clara, CA, 2009.
[10] B. D. Braaten, M. Reich, and J. Glower, "A compact meander-line UHF RFID tag antenna loaded with elements found in right/left-handed coplanar waveguide structures," *IEEE Antennas Wireless Propag. Lett.*, vol. 8, pp. 1158–1161, 2009.
[11] B. D. Braaten, "A novel compact UHF RFID tag antenna designed with series connected open complementary split ring resonator (OCSRR) particles," *IEEE Trans. Antennas Propag.*, vol. 58, no. 11, pp. 3728–3733, 2010.